

## Analysis of Fracture Initiation Pressure of Horizontal Well at Anisotropic Formation Using Boundary Element Method

ZHONG Guanyu<sup>[a],\*</sup>; WANG Ruihe<sup>[a]</sup>; ZHOU Weidong<sup>[a]</sup>; WAN Chunhao<sup>[a]</sup>; CHEN Guichun<sup>[a]</sup>

<sup>[a]</sup> School of Petroleum Engineering, China University of Petroleum (East China), Qingdao, China.

\*Corresponding author.

Received 29 January 2016; accepted 23 February 2016  
Published online 31 March 2016

### Abstract

With the influence of bedding plane, the mechanical properties of bedded rocks, such as shale and coal rock at vertical and parallel bedding direction show comparatively significant difference. Therefore, compared with homogeneous rocks, bedded rocks exhibit obvious anisotropic mechanical properties. Currently, most fracture initiation pressure prediction models simplify rock to homogeneous dielectric elastomer, which is inapplicable to calculate wellbore fracture initiation pressure at bedded stratum. Given that the mechanical properties of bedded rocks at bedding plane direction are the same, this paper established a calculation model of horizontal well fracture initiation pressure in the anisotropic formation and set up a numerical solution method of circumferential stress around the borehole by means of using boundary element method. In addition, a calculation method for fracture initiation pressure based on tensile strength criterion and simplex algorithm was also proposed. The research results indicate that: In the case of high elasticity modulus anisotropy ratio, the wellbore fracture initiation pressure is low; when the elasticity modulus at vertical bedding direction is greater than that at parallel bedding direction, fracture initiation pressure decreases with the increase of bedding dip angle; the shape of wellbore has imposed a significant influence on fracture initiation pressure. For non-circular wellbore, fracture initiation pressure increases with the increase of length-width ratio in the case of smaller ovality. When wellbore shape transforms from equiaxial circle to long and narrow ellipse, fracture initiation pressure decreases with the increase of stress concentration level. Thus, this paper performed calculation

and comparison with classical solutions for particular cases similar to isotropic body of stratum using the model established which verified the validity of the proposed theory. According to the research results, a new method for precise calculation of fracture initiation pressure of horizontal well at bedded stratum was provided.

**Key words:** Horizontal well; Fracture initiation pressure; Anisotropy; Boundary element method

Zhong, G. Y., Wang, R. H., Zhou, W. D., Wan, C. H., & Chen, G. C. (2016). Analysis of fracture initiation pressure of horizontal well at anisotropic formation using boundary element method. *Advances in Petroleum Exploration and Development*, 11(1), 1-9. Available from: URL: <http://www.cscanada.net/index.php/aped/article/view/8171> DOI: <http://dx.doi.org/10.3968/8171>

### INTRODUCTION

Unconventional gas resource is considered as the priority of the development of oil and gas industry in the future. At present, it has become an important and indispensable supplement to conventional oil and gas resource<sup>[1]</sup>. Shale gas and coalbed methane are vital constituent parts of unconventional oil and gas resource. By making comparison with conventional gas reservoir, the permeability of shale gas and coalbed methane reservoir is extremely low. Consequently, industrial airflow can be obtained through hydrofracture<sup>[2]</sup>.

Shale and coal rock have obvious sedimentary structure. Being affected by bedding plane, the elasticity modulus and Poisson's ratio at vertical bedding direction are quite different from that at parallel bedding direction. However, the mechanical properties at all directions parallel to bedding (namely, the so called transverse) are relatively similar. It can be approximately believed as the same. Therefore, shale and coal rock can be deemed as transverse isotropic bodies with isotropic planes<sup>[3]</sup>. Nevertheless, most of the existing fracture initiation

pressure prediction models are based on the assumption that the rock is a homogeneous dielectric elastomer. As a result, it is not applicable to hydraulic fracture treatment design of coalbed methane and shale gas reservoir. In order to accurately predict coalbed methane and fracture initiation pressure of shale gas reservoir, the consideration of anisotropic characteristics of the stratum is required.

With the aim to solve the problem, many scholars carried out researches on wellbore fracture initiation pressure at anisotropy stratum. Lekhniskii et al.<sup>[4]</sup> and Adanoy et al.<sup>[5]</sup> adopted complex variables functions method to deduce stress distribution around the hole based on the theory of anisotropic elasticity. Ong et al.<sup>[6]</sup> analyzed hydrofracture fracture initiation pressure of deviated well at transversely isotropic formation by means of adopting research results of Lekhniskii et al.; Serajian et al.<sup>[7]</sup> adopted analytical method to further analyze the changes on the impact of Poisson's ratio anisotropy on fracture initiation pressure; Hou Bin et al.<sup>[8]</sup> studied the influencing rule of bedding features of coal rock on fracture initiation pressure combined with indoor experiments. Haiyan Zhu et al.<sup>[9]</sup> analyzed stress distribution around the wellbore under the condition of perforation at shale stratum through analytical method. Due to limitation of analytical method, the above calculation assumes wellbore shape to equiaxial circle which is not suitable for the practical situation.

Some scholars studied fracture initiation pressure prediction for horizontal well at anisotropy stratum through numerical algorithm. Yi Wang et al.<sup>[10]</sup> calculated stress distribution on the wellbore hole at carbonatite and other rock stratum under anisotropic elastic modulus using finite element method; Yumei Li et al.<sup>[11]</sup> analyzed fracture initiation pressure at transversely isotropic formations through finite element method; Sitharam Thallak et al.<sup>[12]</sup> studied crack characteristics at anisotropic formation by using particle flow method. It is noteworthy that it is relatively difficult to perform mesh dividing since wellbore is quite small when compared with infinite formation, which is particularly serious in the case of irregular wellbore shape. In addition, the finite element method and discrete element method calculation rely on commercial software. Therefore, its application is limited on site.

Boundary element method is a new numerical method developed after finite element method. Being different from dividing elements in continuum field of finite element method, boundary element method is to divide the elements on the boundary of definitional domain and thus to satisfy control equation and approximate boundary conditions. Therefore, boundary element method is characterized of lower difficulty of mesh dividing, simple data preparation compared with finite element and discrete element method. When compared with analytical method, it has wider applicability. Based on this aim, the author established

a prediction model of horizontal well fracture initiation pressure considering stratum anisotropy on the basis of studying mechanical characteristics of transverse isotropy as well as analyzed the influencing rule of mechanical properties of anisotropy, wellbore shape and geostress on fracture initiation pressure so as to provide a new method for the prediction of wellbore fracture initiation pressure in the process of laminated sedimentary formation.

## 1. PRINCIPLE OF BOUNDARY ELEMENT METHOD

### 1.1 Fundamental Equation of Anisotropy Elastic Mechanics

Balance equation:

$$\sigma_{ij,j} + f_i = 0. \quad (1)$$

Where,  $\sigma_{ij}$  is stress vector component.  $i$  indicates exterior normal at coordinate surface of stress component.  $j$  refers to the direction of stress component.  $f_i$  is physical component and  $i$  indicates the direction of physical component.

Geometric equation:

$$\varepsilon_{ij} = \frac{1}{2} \left( \frac{\partial u_i}{\partial u_j} + \frac{\partial u_j}{\partial u_i} \right). \quad (2)$$

Where,  $\varepsilon_{ij}$  is strain component and  $u_i$  is displacement component.

Constitutive equation

$$\varepsilon = H\sigma. \quad (3)$$

Where,  $H$  is flexibility matrix. For transverse isotropy medium, when symmetry axis coincides with  $Z$  axis, the elasticity modulus  $E_x=E_z=E$  and Poisson's ratio  $\nu_{xz}=\nu$  in isotropic plane,  $E_y=E'$  and  $\nu_{yz}=\nu_{yx}=\nu'$  perpendicular to isotropic plane. Then Equation (3) can be presented as follows:

$$\begin{bmatrix} \varepsilon_x \\ \varepsilon_y \\ \varepsilon_z \\ \gamma_{yz} \\ \gamma_{xz} \\ \gamma_{xy} \end{bmatrix} = \begin{bmatrix} \frac{1}{E} & -\frac{\nu'}{E'} & -\frac{\nu}{E} & 0 & 0 & 0 \\ -\frac{\nu'}{E'} & \frac{1}{E'} & -\frac{\nu'}{E'} & 0 & 0 & 0 \\ -\frac{\nu}{E} & -\frac{\nu'}{E'} & \frac{1}{E} & 0 & 0 & 0 \\ 0 & 0 & 0 & \frac{1}{E} + \frac{1}{E'} + 2\frac{\nu'}{E'} & 0 & 0 \\ 0 & 0 & 0 & 0 & 2\left(\frac{1}{E} + \frac{\nu}{E}\right) & 0 \\ 0 & 0 & 0 & 0 & 0 & \frac{1}{E} + \frac{1}{E'} + 2\frac{\nu'}{E'} \end{bmatrix} \begin{bmatrix} \sigma_x \\ \sigma_y \\ \sigma_z \\ \tau_{yz} \\ \tau_{xz} \\ \tau_{xy} \end{bmatrix}. \quad (4)$$

Where in the Equation (4), flexibility matrix  $H$  is based on the circumstance of coincidence of material coordinate system ( $X', Y', Z'$ ) and global coordinate system ( $X, Y, Z$ ). If global coordinate system is not in line with material coordinate system, flexibility matrix can be transformed to global coordinate system through Equation (5):

$$H = QH'Q^T. \quad (5)$$

Where,  $Q$  is coordinate-transformation matrix. Specific form is as shown in the literature<sup>[13]</sup>.

For issues on the plane problem, Equation (4) can be simplified to<sup>[14]</sup>:

$$\begin{bmatrix} \varepsilon_x \\ \varepsilon_y \\ \gamma_{xy} \end{bmatrix} = \begin{bmatrix} \beta_{11} & \beta_{12} & \beta_{16} \\ \beta_{21} & \beta_{22} & \beta_{26} \\ \beta_{31} & \beta_{32} & \beta_{36} \end{bmatrix} \begin{bmatrix} \sigma_x \\ \sigma_y \\ \tau_{xy} \end{bmatrix}. \quad (6)$$

Where, the expression equation of  $\beta$  is:

$$\beta_{ij} = \begin{cases} a_{ij} & \text{(plane stress)} \\ a_{ij} - \frac{a_{i3}a_{j3}}{a_{33}} & \text{(plane strain)} \end{cases}. \quad (7)$$

Static boundary condition is as follows:

$$p_i = \sigma_{ij}n_j. \quad (8)$$

Where,  $n_j$  refers to included angle between normal line beyond static boundary and  $j$  direction.

Displacement boundary condition is as follows:

$$u_i = \bar{u}_i. \quad (9)$$

Where,  $\bar{u}_i$  is the given displacement boundary condition.

## 1.2 Boundary Element Solution Method

According to reciprocal principle<sup>[15]</sup>, boundary integral equation at boundary points of transverse isotropic elastic body can be solved as follows:

$$\frac{u_i}{2} + \int_{\Gamma} T_{ij}u_j d\Gamma = \int_{\Gamma} U_{ij}p_j d\Gamma. \quad (10)$$

Where, when unit concentration force exists at certain point  $(x_0, y_0)$  at the direction of  $j$  at infinite plane elastic body,  $U_{ij}$  and  $T_{ij}$  are displacement component and stress component of any point  $(x_k, y_k)$  at the direction of  $i$  respectively as<sup>[16]</sup>:

$$U_{ji}(z_k, z_0) = 2\text{Re}[P_{i1}A_{j1}\log(z_1 - z_0) + P_{i2}A_{j2}\log(z_2 - z_0)]. \quad (11)$$

$$T_{ji}(z_k, z_0) = 2\text{Re}\left[\frac{Q_{i1}(\mu_1 n_1 - n_2)A_{j1}}{(z_1 - z_0)} + \frac{Q_{i2}(\mu_2 n_1 - n_2)A_{j2}}{(z_2 - z_0)}\right]. \quad (12)$$

Where,

$$z_k = x_k + \mu_k y_k, \quad (13)$$

$$\begin{cases} P_{1k} = a_{11}\mu_k^2 + a_{12} - a_{16}\mu_k \\ P_{2k} = a_{12}\mu_k^2 + a_{22}/\mu_k - a_{26} \end{cases}, \quad (14)$$

$$Q = \begin{bmatrix} \mu_1 & \mu_2 \\ -1 & -1 \end{bmatrix}, \quad (15)$$

$$\begin{bmatrix} 1 & -1 & 1 & -1 \\ \mu_1 & -\bar{\mu}_1 & \mu_2 & -\bar{\mu}_2 \\ P_{11} & -\bar{P}_{11} & P_{12} & -\bar{P}_{12} \\ P_{21} & -\bar{P}_{21} & P_{22} & -\bar{P}_{22} \end{bmatrix} \begin{bmatrix} A_{j1} \\ \bar{A}_{j1} \\ A_{j2} \\ \bar{A}_{j2} \end{bmatrix} = \begin{bmatrix} \frac{\delta_{j2}}{2\pi i} \\ -\frac{\delta_{j1}}{2\pi i} \\ 0 \\ 0 \end{bmatrix}. \quad (16)$$

Where,  $\mu_k$  is a characteristic value which is related to anisotropic elastic parameters of the material.

In order to improve computational accuracy, perform discretization for the boundary by adopting secondary-unit. And then Equation (10) can be transformed to:

$$\frac{u_i}{2} + \sum_{k=1}^N \sum_{l=1}^3 \left( \int_{\Gamma_k} T_{ij}\phi_l d\Gamma \right) u_j^{kl} = \sum_{k=1}^N \sum_{l=1}^3 \left( \int_{\Gamma_k} U_{ij}\phi_l d\Gamma \right) p_j^{kl}. \quad (17)$$

Where,  $\phi_l$  is the quadratic interpolation function of the unit  $k$  and node 1.  $N$  is the number of boundary elements.

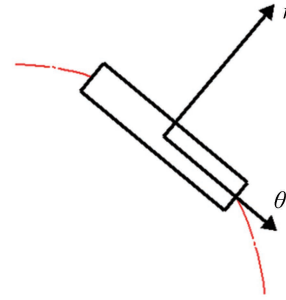


**Figure 1**  
**The Sketch of Local Coordinate System**

According to Figure 1, introduce the local coordinate system for each boundary cell. Then Equation (17) can be rewritten to as follows:

$$\frac{l_{im}^q u_m}{2} + \sum_{k=1}^N \sum_{l=1}^3 \left( \int_{\Gamma_k} T_{ij}\phi_l d\Gamma \right) l_{im}^q u_m^{kl} = \sum_{k=1}^N \sum_{l=1}^3 \left( \int_{\Gamma_k} U_{ij}\phi_l d\Gamma \right) l_{im}^q p_m^{kl}. \quad (18)$$

Where  $l_{im}^q$  is the Cosine of the included angle between global coordinate system at the direction of  $i$  and local coordinate system  $q$  at the direction of  $m$ .

According to Equation (18), displacement and surface force distribution of boundary elements can be derived by combining known boundary conditions.

For the calculation of horizontal well fracture initiation pressure, it is necessary to work out the circumferential stress at wellbore. According to Equation (8), normal component  $\sigma_r$  and tangential component  $\tau_{r\theta}$  can be obtained on wellbore boundary. However, circumferential stress on the boundary cannot be obtained directly from surface force. Thus, it is analyzed by means of adopting physical equation.

According to Equation (5), equation flexibility can be transformed to coordinate system  $\theta$ - $r$  of boundary elements. Based on (6), it can be calculated that:

$$\sigma_\theta = \frac{1}{\beta_{11}'} \left( \frac{\partial u_\theta}{\partial t} - \beta_{12}' \sigma_r - \beta_{16}' \tau_{r\theta} \right). \quad (19)$$

Where,  $\sigma_\theta$  is circumferential stress;  $\beta_{11}'$ ,  $\beta_{16}'$  and  $\beta_{12}'$  are the elements of flexibility matrix under local coordinate system;  $t$  is circumferential length.

Since  $u_\theta$  has been solved out on the boundary, partial derivative  $\partial u_\theta / \partial t$  can be obtained by using

central difference method. Substitute the derived partial derivative, normal and tangential stress components to Equation (19). Circumferential stress distribution can be derived combined with far field geostress conditions.

## 2. COMPUTATIONAL METHOD OF STRATUM FRACTURE INITIATION PRESSURE

### 2.1 Modeling

In order to facilitate the research, a global coordinate system  $XYZ$  based on the direction of geostress was established. Direction  $X$  is the direction of maximum horizontal stress;  $Y$  is the direction of vertical principal stress; and  $Z$  is the direction of minimum horizontal stress; establish local coordinate system  $X'Y'Z'$ . The plane  $X'Z'$  is the bedding plane. The model sketch of is shown in Figure 2.

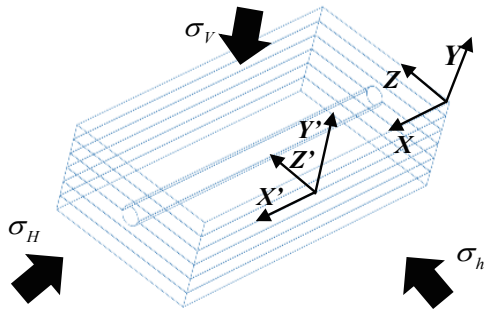


**Figure 2**  
The Sketch of Transversely Isotropic Formation

For thousands of meters long horizontal hole, longitudinal strain at axial direction can be approximately believed as a constant. Consequently, fracturing initiation pressure prediction for horizontal well can be considered as a plane strain issue so as to simplify a complicated three-dimensional stress analysis issue to plane strain issue. According to Figure 3, stratum with unit thickness along wellbore axial direction was analyzed to establish fracture initiation pressure calculation model of horizontal well fracturing.

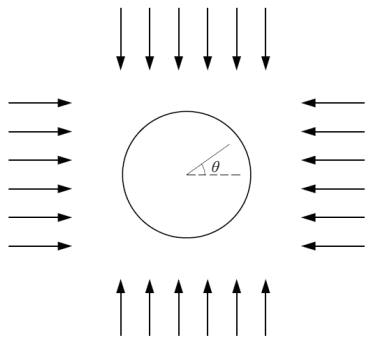


**Figure 3**  
The Sketch of Wellbore Model

To simplify the model, the following assumptions are presented:

(a) Variation of mechanical properties arising from rock and chemical effects of fracturing fluid should not be considered.

(b) Wellbore is a horizontal open hole.

(c) Since mechanical properties at all directions of parallel bedding are relatively approximate, the dynamic property difference at vertical bedding direction and parallel bedding direction is high. Consequently, bedded rock is simplified to transverse isotropy medium taking bedding plane as isotropic plane.

### 2.2 Method to Calculate Formation Pressure Based on Simplex Algorithm

So far, there are a variety of judging criteria about rock cracking. Many scholars<sup>[17-19]</sup> believe that wellbore fracture initiation pressure predicted based on tensile strength criterion is more accurate compared to other fracture criterions. As a result, tensile strength criterion is adopted in this paper to analyze fracture initiation pressure of transversely isotropic formation. The criterion believes that when the maximum circumferential stress at wellbore equals tensile strength of rock, rocks will be subject to tensile failure and generating crack which can be expressed in mathematical expression as follows:

$$\sigma_{\theta_{\max}} + \alpha p_p = S_t \quad (20)$$

Where,  $\sigma_{\theta_{\max}}$  is the maximum circumferential stress around the wellbore;  $S_t$  is tensile strength of rock,  $\alpha$  is Biot coefficient. When the rock is impermeable,  $\alpha=0$ ,  $p_p$  is the pore pressure.

Circumferential stress on the wellbore is the result of joint action of far field stress, wellbore pressure and rock elastic anisotropy, namely:

$$\sigma_{\theta_{\max}} = F(E, E', \nu, \nu', \sigma_{\infty}, p) \quad (21)$$

Where,  $\sigma_{\infty}$  is far field geostress, and  $p$  is wellbore pressure.

Since elastic anisotropy and far field geostress of rock stratum are known conditions, Equation (21) can be further simplified to as follows:

$$F(E, E', \nu, \nu', \sigma_{\infty}, p) = f(p) = S_t - \alpha p_p \quad (22)$$

The solution of Equation (22) is a high nonlinear problem, which can hardly realize solution of Equation (22) by means of analytic calculation. Simplex algorithm is a frequently applied optimization method in recent years. Its primary idea is that: Simplex can be formed with  $n+1$  peak points in  $n$  dimensional space. Besides, change simplex vertices continuously so that simplex objective function can develop to the minimum direction<sup>[20]</sup>. By making comparison with other algorithms, simplex algorithm is simple while the applicability is strong. The equation can be derived with differential coefficient directly. Consequently, it has superiority on nonlinear equation solution. Therefore, solution problem of Equation (22) can be transformed to unconstrained optimization.

The optimal solution can be applied with simplex algorithm so as to solve fracture initiation pressure. The specific flow is as follows:

(a) Establish an objective function:

$$\begin{cases} \min M \\ M(p) = (f(p) - S_t + \alpha p_p)^2 \end{cases} \quad (23)$$

Assume two sets of wellbore pressure as original value to form element shape.

(b) Calculate function values to determine the highest point (maximum value of function  $M$  value) and the lowest point (minimum value of function  $M$  value).

(c) Perform reflection, expansion and compression, rotation and other operations<sup>[21]</sup> on individuals involved to realize optimizing. Operate on the highest point by utilizing simplex algorithm to make the highest point get close to the lowest point, and forcibly develop it to the optimal point area.

(d) Calculate the function values of each point. After reaching the objective precision, the simplex will stop calculating. At this moment, the lowest point of simplex is the optimal solution searched, namely, fracture initiation pressure of horizontal well at transversely isotropic formation; if it cannot satisfy the condition, skip to step (b).

### 2.3 Model Verification

When the elasticity modulus and Poisson's ratio at vertical bedding direction are approximately equal to that at parallel bedding direction, the bedding formation at anisotropic formation can be analyzed as isotropic homogeneous medium. Till now, Fracture initiation pressure of homogeneous rock has attracted the attention

of many scholars<sup>[22-24]</sup>. Therefore, to verify the correctness of aforementioned model and calculation method, this paper calculated under specific condition of isotropic formation by adopting the established model and performed comparison with classical solutions.

Parameter selected in the numerical example is: The elasticity modulus is 35 GPa and the Poisson's ratio is 0.3. The tensile strength of rock is 8 MPa. The maximum horizontal stress is 47.2 MPa. The minimum horizontal stress is 41.6 MPa. The vertical stress is 57.4 MPa. Besides, the rock is impermeable one. In order to avoid singular value, the value of rock mechanics parameters at numerical calculation is:  $E = E' = 35$  GPa,  $\nu = 0.3$ , and  $\nu' = 0.2999$ . Calculate by the aforementioned method. The algorithm process is shown in Figure 4. The calculated fracture initiation pressure of circular wellbore is 75.2 MPa. In addition, the fracture initiation pressure of eclipse wellbore is 82.8 MPa. The theoretical solution of fracture initiation pressure of circular wellbore is 75.4 MPa. And that of eclipse wellbore is 82.91 MPa. Thus, it can be seen that the calculation result of boundary element method is consistent with analytical solution results.

Based on the Figure 5, numerical calculation result is close to analytical solution which further verifies the accuracy of the established model. It can be seen from the Figure that the maximum circumferential stress is  $\theta = 90^\circ$  or  $270^\circ$ , namely, the highest and lowest point of wellbore at vertical stress direction. Therefore, on the basis of the maximum tensile stress criterion, fractures which are created hydraulically are more likely to generate original cracks along with the direction of maximum stress which is in accordance with previous research results<sup>[25]</sup>.

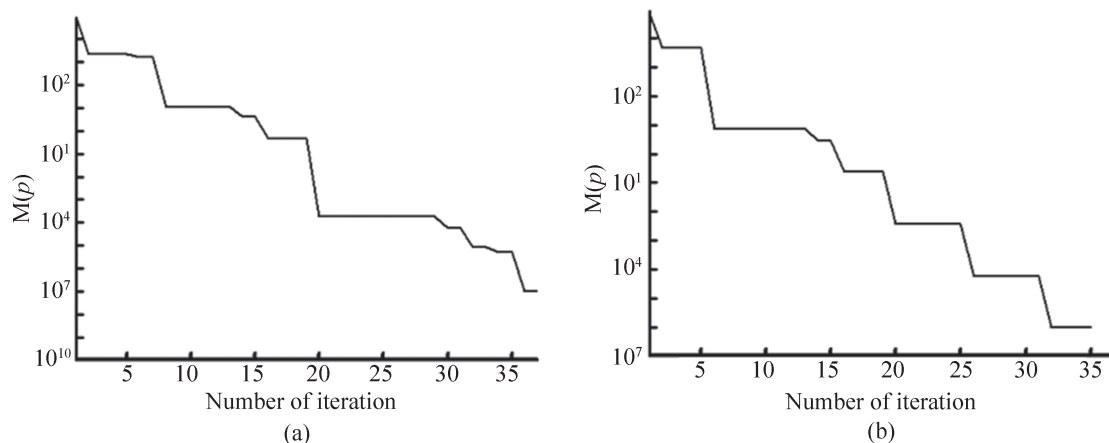


**Figure 4** Convergence Curves for Function. (a) Circle, (b) Eclipse

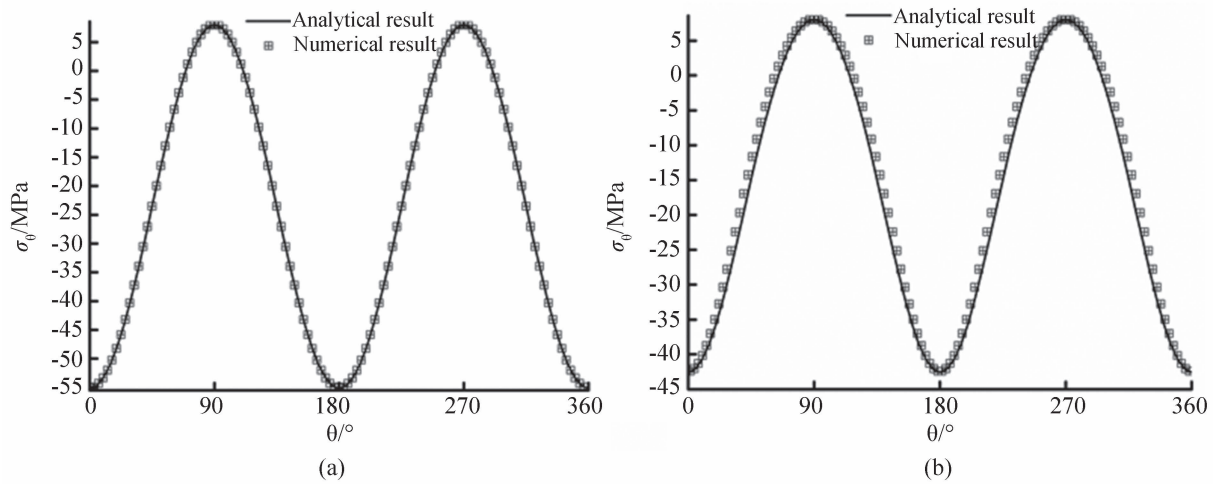


**Figure 5**  
The Distribution of Stress Around the Wellbore. (a) Circle, (b) Eclipse

### 3. EFFECTING FACTORS ANALYSIS

To explore the influencing factors of fracture initiation pressure at transversely isotropic formation, the parameters of certain wall is taken to perform influencing factors analysis. The calculating parameters are shown in Table 1.

**Table 1**  
The Parameters for Simulation

Variable	Value
$E/\text{GPa}$	0.8
$E'/\text{GPa}$	1.6
$\nu$	0.2
$\nu'$	0.4
Tensile strength /MPa	0.8

#### 3.1 Effect of Elastic Anisotropy on Fracture Initiation Pressure

Figure 6 presented the effect of elastic anisotropy on fracture initiation pressure of horizontal well. In the figure,  $K_E$  is defined as the ratio between the elasticity modulus

at parallel bedding direction and that at vertical bedding direction. Obviously, when  $K_E$  is close to 1, the elasticity modulus of rock is close to isotropy. Therefore, it can be seen from the figure that with the increase of ratio, fracture initiation pressure decreases. The reason is that with the increase of  $K_E$ , elasticity modulus at parallel bedding direction will increase relative to that at vertical bedding direction. When the elasticity modulus at vertical bedding direction is small, “mattress effect” will be generated to vertical far field stress, which means that stress diffusion effect is generated at overlying rock stratum, and vice versa. Thus, fracture initiation pressure decreases with the increase of the ratio. Besides, it can also be seen from the figure that when the ratio  $K_E$  is greater than 2, fracture initiation pressure decreases about 3 MPa compared to that calculated at  $K_E = 1$ . So, for rock stratum with strong elastic anisotropy characteristics and the effect of elastic anisotropy on design parameter must be taken into consideration in hydrofracture engineering design.

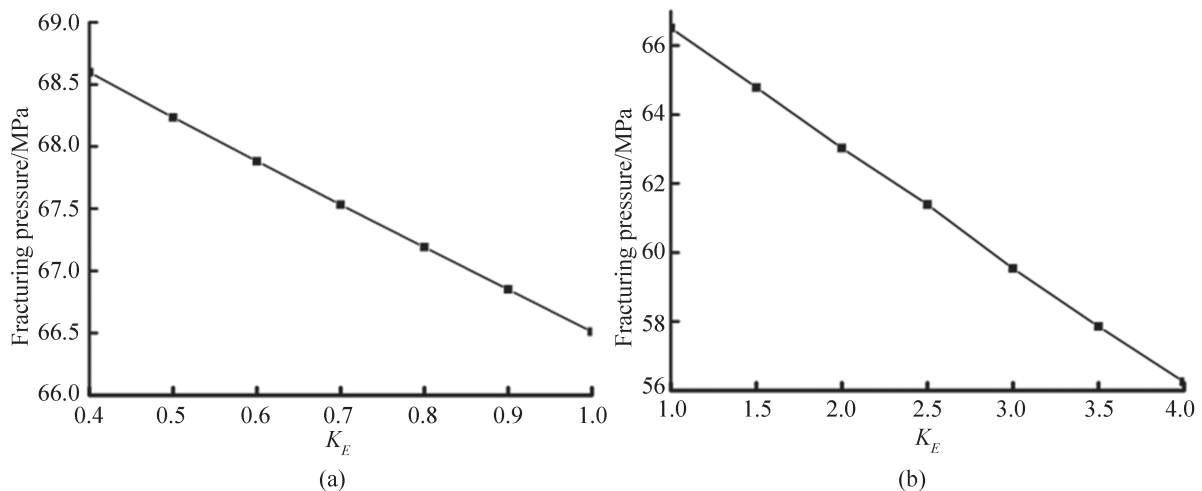


**Figure 6**  
The Effect of Elastic Anisotropy on Fracture Initiation Pressure. (a)  $K_E < 1$ , (b)  $K_E > 1$

### 3.2 Effect of Wellbore Shape on Fracture Initiation Pressure

According to previous researches, wellbore has been simplified to equiaxial circle. However, it is not consistent with actual situation on site<sup>[26]</sup>. Based on this aim, this paper adopted Simsek wellbore model to analyze the effect rules of shape parameter of wellbore on horizontal well fracture initiation pressure at anisotropic formation.

Simsek et al.<sup>[27]</sup> defined the radius of wellbore as follows:

$$R=R_{\text{circle}}(1+\varepsilon\cos^m\theta). \quad (24)$$

Where,  $R_{\text{circle}}$  is the shortest axial length of wellbore  $\varepsilon$  and  $m$  are model parameters.

Figure 7(a) is the effect rule of wellbore shape parameter  $\varepsilon$  on fracture initiation pressure under Simsek wellbore model. Wellbore configuration with different shape parameters  $\varepsilon$  are as shown in Figure 7(b). It can be seen from the Figure that the length-width ratio increases with the increase of  $\varepsilon$ . It has been detected that when the wellbore ovality is low. The fracture initiation pressure increases with the increase of length-width ratio. It is because that the maximum circumferential stress is at  $\theta = 90^\circ$  or  $270^\circ$ . With the increase of  $\varepsilon$ , the radius of curvature at the maximum circumferential stress of wellbore will increase and thus to reduce the stress concentration degree of wellbore, and increase the difficulty of cracking at wellbore.

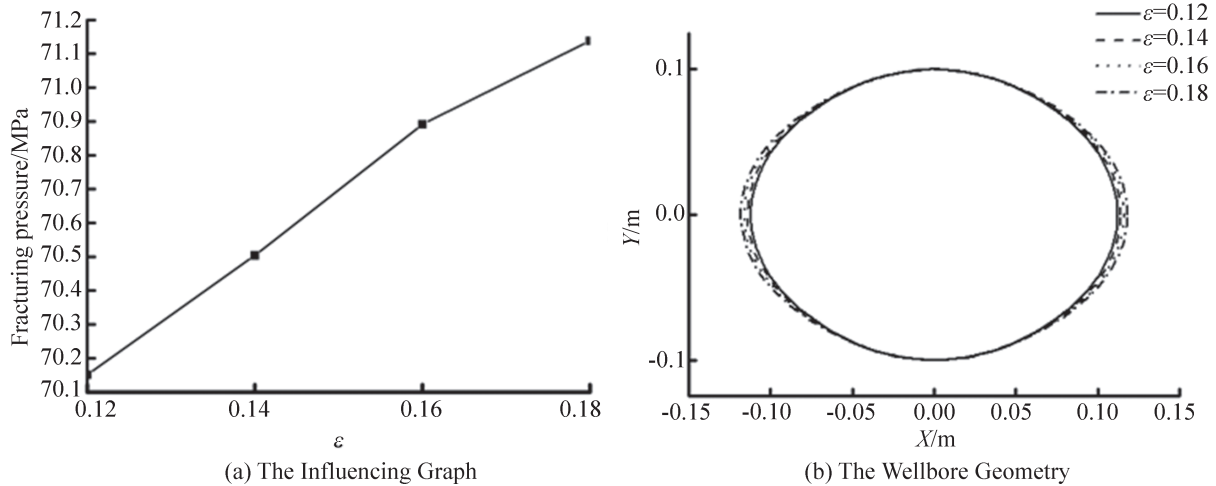


**Figure 7**  
**The Effect of Parameter on Fracture Initiation Pressure**

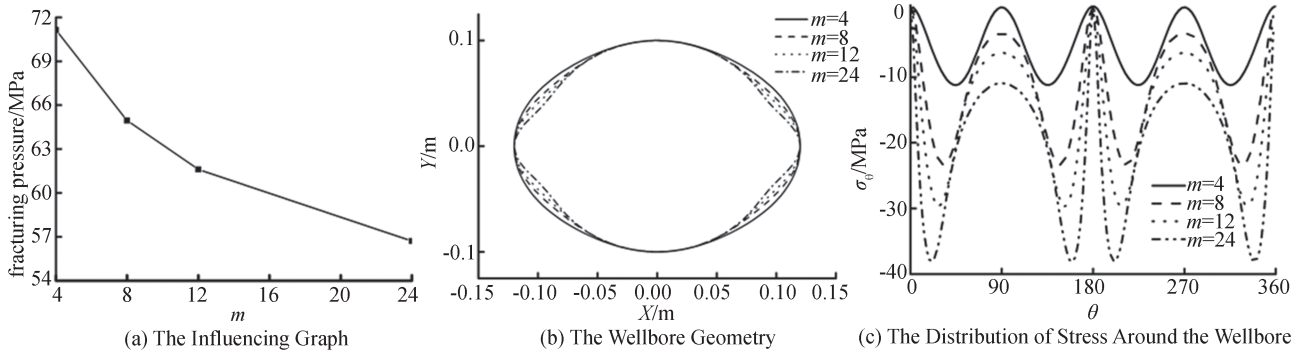


**Figure 8**  
**The Effect of Parameter on Fracture Initiation Pressure**

As shown in Figure 8(a), fracture initiation pressure decreases with the increase of parameter  $m$ . It is because that with the increase of  $m$ , wellbore shapes at horizontal direction change from equiaxial circle to long and narrow ellipse which lead to serious stress concentration. Consequently, when parameter  $m$  is high as shown in

Figure 8(c), the position of the maximum circumferential stress transfers from  $\theta = 90^\circ$  or  $270^\circ$  to  $\theta = 0^\circ$  or  $180^\circ$ . Significant stress concentration can be observed at the horizontal direction. Stress concentration degree aggravate with the increase of parameter  $m$ . Therefore, fracture initiation pressure significantly decreases.

### 3.3 Effect of Rock Bedding Dip Angle on Fracture Initiation Pressure

According to the figure with the increase of rock bedding dip angle, fracture initiation pressure decreases. Based on coordinate transformation equation of flexibility matrix<sup>[29]</sup>, if the elasticity modulus at vertical bedding direction is greater than that at parallel bedding direction, while the rock bedding dip angle increasing, the elasticity modulus at vertical stress direction will decrease and the elasticity modulus at horizontal stress direction will increase. Thus, stratum present weaker rigidity at vertical direction which greatly reduces cracking difficulty of horizontal. Therefore, when the elasticity modulus vertical to bedding is greater than that parallel to the bedding, the fracture initiation pressure will decrease with the increase of bedding dip angle.

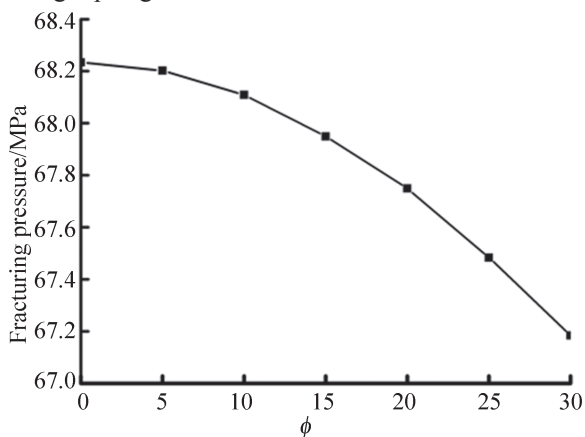


**Figure 9**  
The Effect of Bedding Angle on Fracture Initiation Pressure

## CONCLUSION

(a) Based on anisotropy theory and boundary element method, this paper established a horizontal well fracture initiation pressure calculating model for anisotropic formation. It also put forward calculating method for wellbore circumferential stress by means of boundary element method and proposed fracture initiation pressure calculating method combining with tensile strength criterion and simplex algorithm so as to provide a new method for horizontal well fracture initiation pressure prediction in shale, coal rock as well as other layered rock stratum.

(b) At anisotropic formation, fracture initiation pressure decreases with the increase of elastic anisotropy ratio. When the elasticity modulus vertical to bedding is greater than that parallel to the bedding, the fracture initiation pressure will decrease with the increase of bedding dip angle.

(c) At anisotropic formation, for non-circular wellbore, when the ovality is low, the horizontal well fracture initiation pressure increases with the increase of length-width ratio. When wellbore shape transforms

from equiaxial circle to long and narrow ellipse, fracture initiation pressure decreases with the increase of stress concentration level.

## REFERENCES

- [1] Dong, Z. Z., Holditch, S., McVay, D., & Ayers, W. B. (2012). Global unconventional gas resource assessment. *SPE Economics & Management*, 4(4), 222-234.
- [2] Saldungaray, P. M., & Palisch, T. T. (2012). *Hydraulic fracture optimization in unconventional reservoirs*. Paper presented at the SPE Unconventional Resources Conference, Abu Dhabi, UAE.
- [3] Zamiran, S., Osouli, A., & Ostadhassan, M. (2014). *Geomechanical modeling of inclined wellbore in anisotropic shale layers of Bakken formation*. Paper presented at 48<sup>th</sup> U.S. Rock Mechanics/Geomechanics Symposium, Minneapolis, Minnesota.
- [4] Lekhnitskij, S. G. (1977). *Theory of the elasticity of anisotropic bodies*. Moscow: Mir Publishers.
- [5] Aadnoy, B. S. (1988). Modeling of the stability of highly inclined wellbores in anisotropic rock formations. *SPE Drilling Engineering*, 3(3), 259-268.
- [6] Ong, S. H., & Roegiers, J. C. (1995). *Fracture initiation from inclined wellbores in anisotropic formations*. Paper presented at the International Meeting on Petroleum Engineering, Beijing, China.
- [7] Serajian, V. (2011). *A study of hydraulic fracturing initiation in transversely isotropic rocks* (Doctoral dissertation). Texas A&M University, USA.
- [8] Hou, B., Chen, M., & Wang, Z. (2013). Hydraulic fracture initiation theory for a horizontal well in a coal seam. *Petroleum Science*, 10(2), 219-225.
- [9] Zhu, H. Y., Guo, J. C., & Zhao, X. (2014). Hydraulic fracture initiation pressure of anisotropic shale gas reservoirs. *Geomechanics & Engineering*, 7(4), 403-430.
- [10] Wang, H. Y., Kumar, A., & Samuel, R. (2014). *Geomechanical modeling of wellbore stability in anisotropic salt formation*. Paper presented at SPE Latin America and Caribbean Petroleum Engineering Conference, Maracaibo, Venezuela.
- [11] Li, Y. M., Liu, G. H., & Li, J. (2015). Improving fracture initiation predictions of a horizontal wellbore in laminated anisotropy shales. *Journal of Natural Gas Science & Engineering*, 24, 390-399.
- [12] Thallak, S., Rothenburg, L., & Dusseault, M. (1991). *Simulation of multiple hydraulic fractures in a discrete element system*. Paper presented at the 32<sup>nd</sup> U.S. Symposium on Rock Mechanics (USRMS), Norman, Oklahoma.
- [13] Bobet, A., & Yu, H. T. (2015). Stress field near the tip of a crack in a poroelastic transversely anisotropic saturated rock. *Engineering Fracture Mechanics*, 141, 11-18.
- [14] Pan, E., & Amadei, B. (1996). Fracture mechanics analysis of cracked 2-D anisotropic media with a new formulation of the boundary element method. *International Journal of Fracture*, 77(2), 161-174.



- [15] Marques, S. P. C., & Creus, G. J. (2012). *Computational Viscoelasticity* (pp.87-92). Berlin Heidelberg: Springer.
- [16] Ke, C. C., Chen, C. S., & Tu, C. H. (2008). Determination of fracture toughness of anisotropic rocks by boundary element method. *Rock Mechanics & Rock Engineering*, 41(4), 509-538.
- [17] Hossain, M. M., Rahman, M. K., & Rahman, S. S. (2000). Hydraulic fracture initiation and propagation: Roles of wellbore trajectory, perforation and stress regimes. *Journal of Petroleum Science & Engineering*, 27(3), 129-149.
- [18] Huang, J. S., Griffiths, D. V., & Wong, S. W. (2012). Initiation pressure, location and orientation of hydraulic fracture. *International Journal of Rock Mechanics & Mining Sciences*, 49(1), 59-67.
- [19] Guo, J. C., He, S. G., & Deng, Y. (2015). New stress and initiation model of hydraulic fracturing based on nonlinear constitutive equation. *Journal of Natural Gas Science and Engineering*, 27, 666-675.
- [20] Bazaraa, M. S., Sherali, H. D., & Shetty, C. M. (2013). *Nonlinear programming: Theory and algorithms*. New Jersey: John Wiley & Sons.
- [21] Maehara, N., & Shimoda, Y. (2013). Application of the genetic algorithm and downhill simplex methods (Nelder-Mead methods) in the search for the optimum chiller configuration. *Applied Thermal Engineering*, 61(2), 433-442.
- [22] Aadnoy, B., Kaarstad, E., & Aadnoy, B. (2010, November). *Elliptical geometry model for sand production during depletion*. Paper presented at IADC/SPE Asia Pacific Drilling Technology Conference and Exhibition, Ho Chi Minh City, Vietnam.
- [23] Zoback, M. D., Moos, D., & Mastin, L. (1985). Wellbore breakouts and in situ stress. *Journal of Geophysical Research*, 90(b7), 5523-5530.
- [24] Sun, X. Z., & Sun, M. F. (1998). Influence of ovality on wellbore extruding and collapsing destruction. *Journal of Daqing Petroleum Institute*, 22(3), 14-17.
- [25] Haimson, B., & Fairhurst, C. (1967). Initiation and extension of hydraulic fractures in rocks. *Society of Petroleum Engineers Journal*, 7(3), 310-318.
- [26] Kang, Y. F., Yu, M. J., & Miska, S. Z. (2009). *Wellbore stability: A critical review and introduction to DEM*. Paper presented at SPE Annual Technical Conference and Exhibition, New Orleans, Louisiana, USA.
- [27] Şimşek, E., & Sinha, B. K. (2008). Analysis of noncircular fluid-filled wellbores in elastic formations using a perturbation model. *Journal of the Acoustical Society of America*, 124(1), 213-217.
- [28] Wang, H. Y. (2015). Numerical modeling of non-planar hydraulic fracture propagation in brittle and ductile rocks using XFEM with cohesive zone method. *Journal of Petroleum Science & Engineering*, 135, 127-140.
- [29] Sollero, P., & Aliabadi, M. H. (1993). Fracture mechanics analysis of anisotropic plates by the boundary element method. *International Journal of Fracture*, 64(4), 269-284.